

# THERMAL ANALYSIS OF TRANSITION METAL AND RARE EARTH OXIDE SYSTEM-GAS INTERACTIONS BY A SOLID ELECTROLYTE-BASED COULOMETRIC TECHNIQUE

*K. Teske, H. Ullmann and N. Trofimenko*

Institute of Inorganic Chemistry, Dresden Technical University, Germany

## Abstract

The oxidation-reduction behaviour of transition metal and rare earth oxide systems in oxygen potential controlled atmospheres was investigated by means of a solid electrolyte-based coulometric technique (SEC) in carrier gas mode to obtain information concerning the extent of oxygen stoichiometry, the  $p$ - $T$ - $x$  diagram of any mixed oxide phase, the kinetics of the oxygen exchange and the phase transitions.

The direct coupling of SEC and electrical conductivity measurements provides further information about the relationship between oxygen deficiency and conductivity, especially as concerns the oxygen mobility and the transition from ionic to mixed ionic/electronic conductivity in any system.

In the fluorite-type phases  $\text{PrO}_{2-x}$ ,  $\text{Ce}_{0.8}\text{Pr}_{0.2}\text{O}_{y-x}$  and  $\text{Ce}_{0.8}\text{Sr}_{0.08}\text{Pr}_{0.12}\text{O}_{y-x}$ , the higher oxidation state of Pr is stabilized and the electrical conductivity increases in this sequence. The perovskite-type phase  $\text{Sr}_{1-y}\text{Ce}_y\text{FeO}_{3-x}$  shows transitions and a second phase reflected in the temperature-programmed spectrum of this substance. The electrical conductivity of  $\text{Sr}_{0.9}\text{Ce}_{0.1}\text{FeO}_{3-x}$  changes from  $n$ -type to  $p$ -type with increasing oxygen pressure.

**Keywords:** coulometry, electrical conductivity, mixed oxides, oxygen stoichiometry,  $p$ - $T$ - $x$  diagram, solid electrolyte

## Introduction

Mixed transition and rare earth oxides with a more or less wide range of oxygen nonstoichiometry are of interest as candidate materials with catalytic activity, as solid-state electronics and ionics, for electrodes or electrolytes in solid oxide sensors or fuel cells, and as superconductors, magnetic materials or oxygen-permeable membranes. These characteristics depend on chemical and phase compositions and temperature, as well as on the oxidation state and oxygen transfer properties of the mixed oxides.

The oxidation-reduction behaviour of such transition metal systems in oxygen potential controlled atmospheres was investigated by means of a solid electrolyte-based coulometric technique (SEC) in carrier gas mode to obtain information concerning the extent of oxygen stoichiometry, the  $p$ - $T$ - $x$  diagram of any mixed oxide phase, the kinetics of the oxygen exchange and the phase transitions.

A special version of SEC was developed in connection with the temperature- and time-programmed oxygen partial pressure of the reaction gas, derived from the  $p$ - $T$ - $x$  parameters of a sample under investigation.

The earlier work focused mainly on candidate materials for applications as superionic conductors, electrodes in SOFCs [1], superconductors [2, 3] and nuclear fuel materials [4].

The main objective of the present study was to demonstrate the possibilities of SEC for measuring the change in oxygen stoichiometry of oxide powders and ceramic shapes and to investigate the influence of the oxidation state on the phase structure and physical (especially electrical) properties of some chosen mixed oxides ( $Ce_{0.8}Pr_{0.2}O_y$ ,  $Ce_{0.8}Sr_{0.08}Pr_{0.12}O_y$  and  $Sr_{1-y}Ce_yFeO_{3-x}$ ).

## Experimental arrangements

The basic concept of combined coulometric-potentiometric arrangement for the investigation of solid-gas interactions in the carrier gas mode was described earlier [5]. A modified more flexible version, especially for combinations with measurements of electrical conductivity, is shown schematically in Fig. 1.

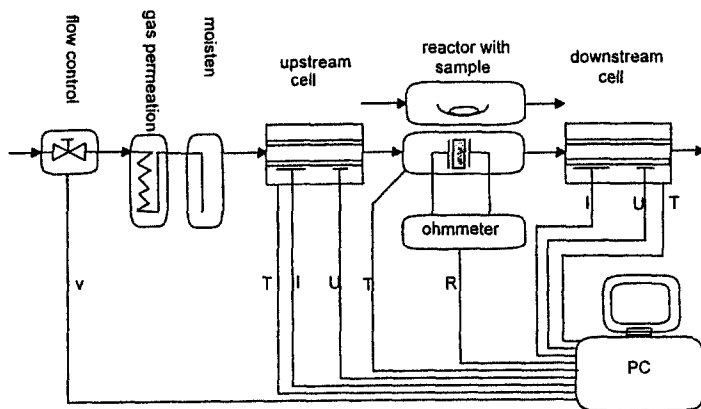


Fig. 1 Schematic view of the experimental set-up with solid electrolyte cells for coulometric-potentiometric measurements in carrier gas mode ( $v$ =gas flow,  $T$ =temperatures,  $I$ =currents,  $U$ =voltages)

The steady-state carrier gas flow of 4–6 l h<sup>-1</sup> could be exactly adjusted as concerns gas concentrations of gas addends and oxygen potential by a permeation device, a moistifier and the upstream solid electrolyte cell. The dosing part of the upstream cell allows control of the oxygen potential as a function of time (stepwise or continuous), the sample temperature or other parameters. The sample under investigation is placed in a quartz tube reactor and heated according to an evaluated program. All changes in concentrations of hydrogen or oxygen and the oxygen potential during the solid-gas interaction are registered continuously in the downstream cell, which is identical in construction to the first one, by coulometric titrations and potentiometric measurements, respectively.

Simultaneous measurements of electrical conductivity are carried out on bar-shaped samples by the 4-wire method in a gastight tube reactor instead of the tube for powder reactions. The contacts are directly incorporated during the preparation of the samples by pressing and tempering.

### Temperature-programmed oxygen desorption (TPD spectra)

TPD experiments in general provide information about characteristic temperatures of a substance connected with structural changes because the mechanism and absolute value for oxygen sorption-desorption are influenced by such transitions. An example is given for the reaction of  $\text{Pr}_6\text{O}_{11}$  in an  $\text{Ar-H}_2\text{-H}_2\text{O}$  mixture. Numerous maxima of oxygen desorption as functions of temperature and oxygen stoichiometry are seen in this spectrum (Fig. 2). The oxygen stoichiometry obtained at a given time (and temperature) after a maximum in oxygen desorption, calculated from the titration current of the downstream cell, is shown in the Figure. Some peaks correlate with well-known praseodymium oxide phases ( $\text{Pr}_n\text{O}_{2n-2}$ ), but there are also peaks that can not be assigned. This complex picture of the TPD spectrum disappears if Pr is incorporated in a mixed oxide structure (see below).

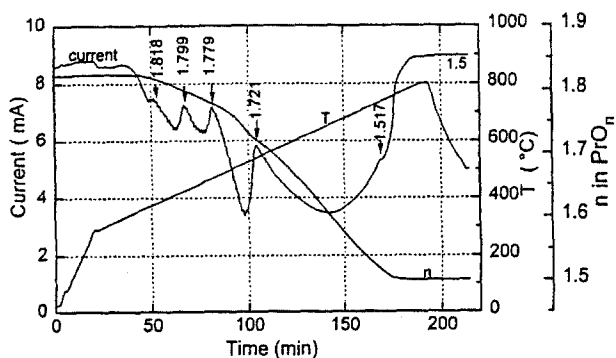


Fig. 2 TPD spectrum of oxygen from  $\text{Pr}_6\text{O}_{11}$  in  $\text{Ar-H}_2\text{-H}_2\text{O}$  ( $p_{\text{H}_2} = 800$  vpm,  $\text{H}_2/\text{H}_2\text{O} = 0.5$ ) (the numbers on the current curve are oxygen stoichiometries reached at this point)

The analysis of the TPD spectra of the perovskite-type phase  $\text{Sr}_{1-y}\text{Ce}_y\text{FeO}_{3-x}$  indicate phase transformations depending on temperature and  $y$ . The desorption spectrum of an air-oxidized sample (Fig. 3) exhibits three peaks: For undoped  $\text{SrFeO}_{3-x}$  ( $y=0$ ), the broad peak between 380 and 600°C reflects the existence of two phases transforming at different temperatures. The smaller peak at 835°C indicates another phase transformation within the perovskite structure. Doping with ceria changes the spectra considerably: Beginning at  $y=0.01$  up to 0.3 mol of ceria, qualitatively identical spectra are observed. At  $y>0.3$ , the spectra differ at higher temperatures ( $>850^\circ\text{C}$ ), indicating some fundamental structural changes. It is known from X-ray data [6] that the limit of existence of the solid solution is reached at about  $y=0.3$ . The maximum oxygen release of all Ce-doped samples, independent of Ce concentration, takes place in the same manner at 400–500°C,

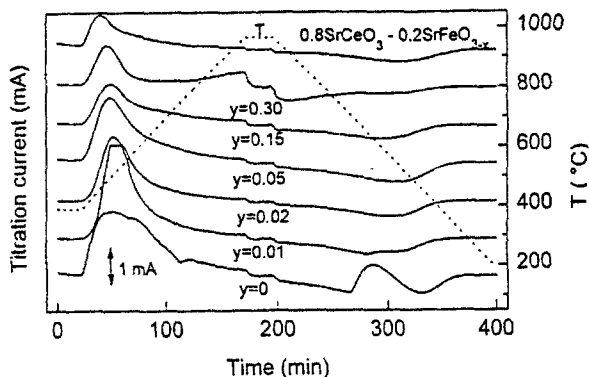


Fig. 3 TPD spectra of perovskite-type phase  $\text{Sr}_{1-y}\text{Ce}_y\text{FeO}_{3-x}$  in  $\text{Ar-H}_2\text{-H}_2\text{O}$  in  $\text{Ar-O}_2$  ( $p_{\text{O}_2} = 10.5$  Pa)

which demonstrates that, even in the two-phase mixture  $0.8\text{SrCeO}_3\text{-}0.2\text{SrFeO}_{3-x}$ , the oxygen-desorbing phase is the solid solution  $\text{Sr}_{1-y}\text{Ce}_y\text{FeO}_{3-x}$ .

### *P-T-x* measurements

For thermodynamic characterization of any mixed oxide, the oxygen exchange up to equilibrium under defined and adjustable conditions in the *p-T-x* space is always of interest. There are three possible versions of measurements with this SEC equipment.

1. Isobar temperature ramping and measurement of the time dependence of oxygen exchange: in this case, the upstream cell may operate in potentiometric or coulometric mode.
2. Isothermal ramping of oxygen pressure by change of the dosing current in the upstream cell.
3. Equilibrated measurements: Measurements of the oxygen potential of any substance can be performed by systematic change of the oxygen potential in the upstream cell, controlling the dosing current in this cell so that the oxygen change between the gas and the sample goes to zero. This may be achieved by comparison of the potential of the upstream cell with that of the downstream cell. The assumptions for this strategy are that the reactivity of the sample is high enough, the gas composition allows change of the oxygen potential in the region in question, and the sample displays a certain buffer capacity for oxygen. In this 'isostiochiometric' version, the equilibrium is faster because no (or very small) oxygen gradients arise during measurements.

If the *p-T-x* function is formulated in a numeric equation, then the oxygen pressure can be controlled by software connecting of the sample temperature and upstream dosing current so that cooling down occurs along an isostiochiometric curve

and no gradient of oxygen arises in the solid. This is of special interest if low-temperature properties are connected with an oxygen deficiency generated at higher temperature (for instance, the superconductivity of oxide ceramics).

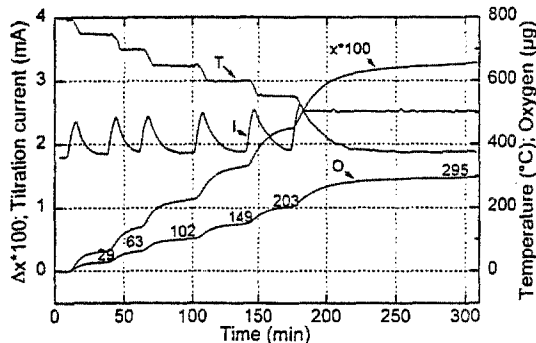


Fig. 4  $T-\Delta x$  measurement at constant  $p$  (version 1) of  $Ce_{0.8}Pr_{0.2}O_{y-x}$  in Ar- $O_2$  ( $p_{O_2} = 10$  Pa)

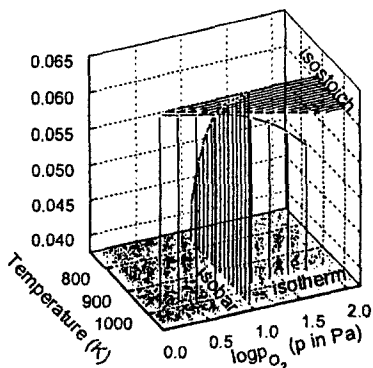


Fig. 5 Isothermal, isobaric and iso stoichiometric SEC measurements in the  $p-T-x$  space of  $Ce_{0.8}Pr_{0.2}O_{y-x}$  (the sample was preheated in air;  $y$  see text)

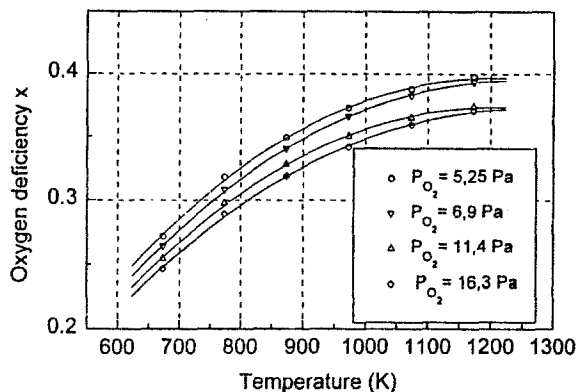


Fig. 6 Oxygen deficiency of  $Sr_{0.9}Ce_{0.1}FeO_{3-x}$  as a function of temperature at different  $p_{O_2}$

For demonstration, these three versions  $p$ - $T$ - $x$  measurements were studied for  $\text{Ce}_{0.8}\text{Pr}_{0.2}\text{O}_{y-x}$  (Figs 4 and 5).

In the oxygen-deficient cubic-type phase  $\text{Ce}_{0.8}\text{Pr}_{0.2}\text{O}_y$  as compared to the pure praseodymium oxides, a higher oxidation state of Pr is stabilized. The oxygen deficiency at 800°C related to an air-oxidized sample at  $6.7 \cdot 10^{-11}$  Pa was found to be 0.094. Since the oxygen deficiency of pure  $\text{CeO}_2$  under these conditions is more than two orders smaller, the change in stoichiometry can be attributed to the Pr giving an oxygen stoichiometry in the mixed oxide of 1.994 and a mean oxidation state for Pr of 1.970. This stabilization effect is more dramatic in the ternary oxide  $\text{Ce}_{0.8}\text{Sr}_{0.08}\text{Pr}_{0.12}\text{O}_y$ , where we found a change in oxygen stoichiometry of 0.058 corresponding to Pr 1.984 under the same conditions. At lower oxygen pressure, the cerium participates measurably in the reduction process (at  $10^{-15}$  Pa, the oxygen deficiency in the two mixed oxides is 0.131 and 0.091, respectively).

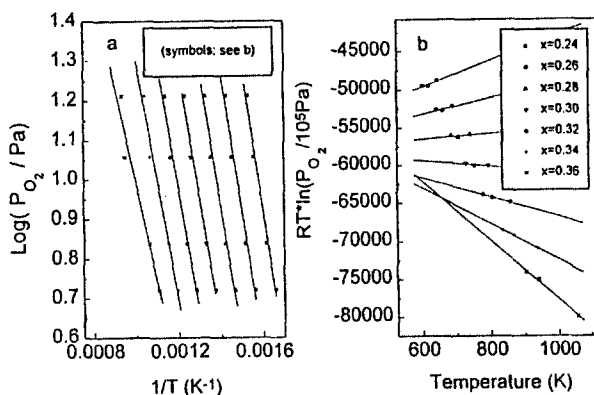


Fig. 7 Equilibrium oxygen pressure vs. inverse temperature (a) and equilibrium oxygen pressure multiplied by temperature vs. temperature (b) at fixed oxygen content in  $\text{Sr}_{0.9}\text{Ce}_{0.1}\text{FeO}_{3-x}$

A further example is given for the perovskite-type phase  $\text{Sr}_{0.9}\text{Ce}_{0.1}\text{FeO}_{3-x}$ . The results measured in the above-described first version at constant oxygen pressure are given in Fig. 6. From the  $p_{\text{O}_2}$ - $T$ - $x$  functions, the thermodynamic stability data of the materials can be calculated. The oxygen deficiency of the materials increases with temperature and with decreasing  $p_{\text{O}_2}$  (Fig. 6). The  $x$  values are related to the oxygen chemical potential  $\mu_{\text{O}}$ , and the slopes of the plots of  $\log p_{\text{O}_2}$  vs.  $1/T$  and  $RT \ln p_{\text{O}_2}$  vs.  $T$  at constant  $x$  give the partial molar enthalpy  $\Delta H_{\text{O}}$  and partial molar entropy  $\Delta S_{\text{O}}$ , respectively (Fig. 7). The plots to a good approximation are straight lines, from which the enthalpy and entropy values can be determined [7].

## Coupling of electrical conductivity measurements and SEC

The electrical conductivity acts as the fourth dimension in the  $p$ - $T$ - $x$ - $\sigma$  space. There are also some versions of measurement:

1. Temperature function of conductivity at constant pressure: in general, for substances with a high range of oxygen non-stoichiometry, the approach to equilibrium is slow, and thus a continuous elevation of temperature creates systematic errors. A stepwise change of temperature by coulometric or potentiometric control of the gas-solid equilibrium is helpful. In this way, information is obtained about  $\Delta x$  and  $\sigma$  simultaneously.

2. Temperature function of  $\sigma$  at constant  $x$ : the method is the same as for  $p$ - $T$ - $x$  measurements (see above). In this way, the influence of stoichiometric change on conductivity is eliminated: the gas and solid are in equilibrium at any time and the time dependence of conductivity is avoided.

3. Pressure function of  $\sigma$  at constant  $T$ : coulometric control of the gas composition in carrier- $O_2$ - $H_2$ - $H_2O$  by the upstream cell, and control of the equilibration by the downstream cell, covers the whole range from  $p_{O_2} = 10^4$  Pa down to  $10^{-20}$  Pa. Examples of these three versions for the mixed conductors  $Ce_{0.8}Pr_{0.2}O_y$  and  $Ce_{0.8}Sr_{0.08}Pr_{0.12}O_y$  are shown in Figs 8, 9 and 10.

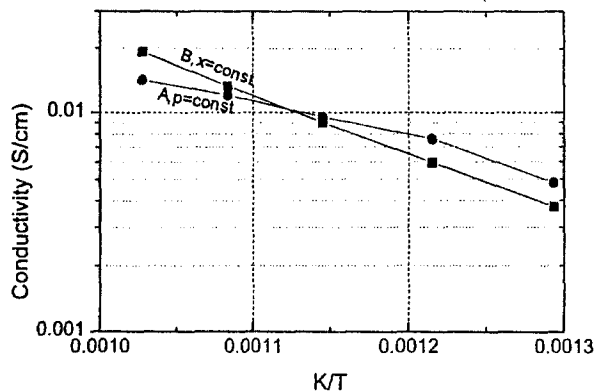


Fig. 8 Temperature dependence of conductivity of  $Ce_{0.8}Pr_{0.2}O_{y-x}$  measured in isobaric (A) or isostoichiometric mode (B)

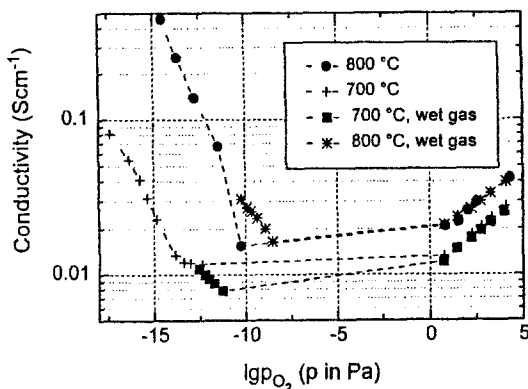


Fig. 9 Pressure function of the conductivity of  $Ce_{0.8}Pr_{0.2}O_{y-x}$  measured in a SEC-controlled  $Ar-O_2$  or  $Ar-H_2-H_2O$  gas flow

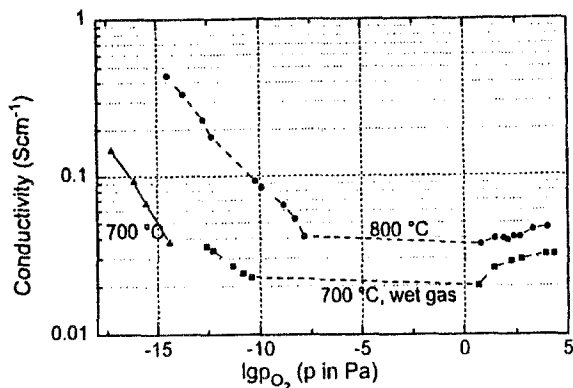


Fig. 10 Pressure function of the conductivity of  $\text{Ce}_{0.8}\text{Sr}_{0.08}\text{Pr}_{0.12}\text{O}_{y-x}$  measured in a SEC-controlled Ar-O<sub>2</sub> or Ar-H<sub>2</sub>-H<sub>2</sub>O gas flow

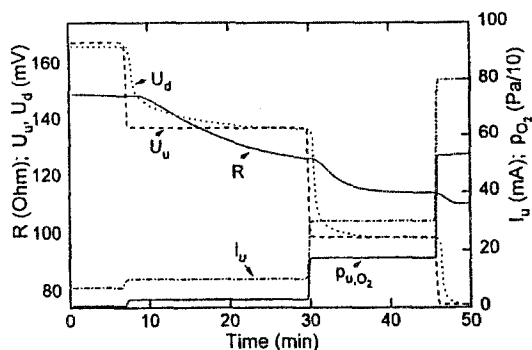


Fig. 11 Change in conductivity of  $\text{Ce}_{0.8}\text{Pr}_{0.2}\text{O}_{y-x}$  and downstream cell potential during ramping of oxygen pressure by upstream current (temperature of sample and SE cell 973 K)

We can not confirm the argumentation of Ma *et al.* [8] that the electrical conductivity is much more sensitive than direct oxygen exchange measurements. An example of the time dependence of the resistance, upstream and downstream cell voltage and oxygen pressure after stepwise switching of the upstream current is demonstrated in Fig. 11. Measurement of oxygen exchange seems to be an acceptable alternative method for determination of the diffusion coefficient of oxygen in such mixed oxides. For more details, see [9].

It is worthy of note that there is a marked difference in the temperature functions of conductivity measured at constant pressure or at constant  $x$ .

In the whole range of oxygen pressure, the conductivity of the Sr-doped mixed oxide is about twice as high as that for the Ce-Pr-O phase. The results for  $\text{Ce}_{0.8}\text{Pr}_{0.2}\text{O}_y$  agree with those measured in air [10]. In the low oxygen pressure region ( $<10^{-10}$  Pa), both substances show a steeper gradient in conductivity. In this



region, the electronic conductivity dominates, whereas at higher oxygen pressure, mixed conduction is expected, with a certain ionic contribution, especially in the Sr-doped phase.

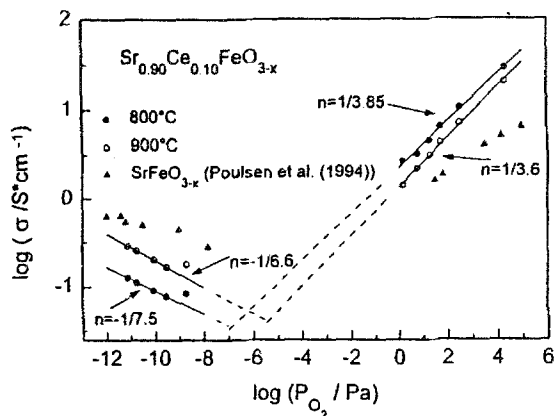


Fig. 12 Specific electrical conductivity of  $\text{Sr}_{0.9}\text{Ce}_{0.1}\text{FeO}_{3-x}$  as a function of oxygen partial pressure  $p_{\text{O}_2}$ .

For the perovskite-type phase  $\text{Sr}_{0.9}\text{Ce}_{0.1}\text{FeO}_{3-x}$ , another shape of the  $\sigma$ - $p$  curve was found. The dependence of the specific conductivity on the  $p_{\text{O}_2}$  values in the surrounding gas (Fig. 12) demonstrates the domination of  $p$ -type conduction within the range of higher oxygen pressure. Under reducing conditions,  $n$ -type conduction appears. Measurements in the transition region are not available because of the absence of gases with stable oxygen partial pressures. Thus, statements on the level of the ionic conductivity are not possible. However, the high level of  $\sigma_n = \sigma_p$  near  $10^{-1} \text{ S cm}^{-1}$  of total conductivity and the suggestion of an oxygen pressure-independent region above  $10^{-14} \text{ atm O}_2$  indicate that the ionic conductivity in this material is of the order of doped  $\text{CeO}_2$  conductivity values [11]. The slopes of  $1/3.8$  for  $p$ -type conduction and  $1/7$  for  $n$ -type conduction cannot easily be assigned to a certain redox reaction because of the complexity of possible oxygen-exchange processes in doped materials. A steeper slope in the  $p$ -type region (nearly  $1/4$ – $1/5$ ) was found for undoped  $\text{SrFeO}_{3-x}$  as well [12].

## Outlook

Many of the physical properties of solid oxides depend on the oxidation state of the oxides. If one physical property has to be investigated in the range of higher temperatures, coupling of SEC with the measurement of the actual physical property is an efficient tool for the attainment of more complex results. As an example, electrical conductivity measurements on oxides are demonstrated in this paper. Coupling of SEC with TGA has started [13].

Simultaneous control and measurement of oxygen potential during X-ray measurement have not yet been achieved. Coupling of SEC with X-ray diffraction would be an efficient tool for investigation of the phase diagrams of oxides and lattice parameters in the  $T$ - $p$ - $x$  space. In this way, SEC offers a broad field for the investigation of inorganic solids.

## References

- 1 K. Teske, E. Syskakis and S. Naoumidis, Proc. 14th Risø International Symposium on Materials Science, Denmark 1993.
- 2 K. Teske, W. Anwand and K. Fischer, *J. Alloys and Compounds*, 195 (1993) 671.
- 3 K. Teske, *Materials Science Forum*, 76 (1991) 269.
- 4 K. Teske, C. Nebelung, H. Ullmann, I. I. Kapshukov, L. V. Sudakov and A. S. Bevz, *J. Nucl. Mater.*, 188 (1992) 226.
- 5 M. Bode, K. Teske and H. Ullmann, *GIT-Fachz. Lab.*, 38 (1994) 495.
- 6 H. Ullmann, N. Trofimenko and J. Paulsen, paper to be presented at 17th Risø International Symposium on Materials Science.
- 7 N. Trofimenko, H. Ullmann, J. Paulsen and R. Müller, *Solid State Ionics*, to be published.
- 8 B. Ma, U. Balchandran, J.-H. Park and C. U. Segre, *Solid State Ionics*, 83 (1996) 65.
- 9 V. V. Vashook, M. V. Zinkevich, H. Ullmann and K. Teske, paper to be presented at 17th Risø International Symposium on Materials Science.
- 10 M. Nauer, Ch. Fükos and B. C. H. Steele, *J. Europ. Ceram. Soc.*, (1994) 493.
- 11 H. Ullmann and K. Teske, 4th Int. Symp. on Systems with Fast Ionic Transport, Warszawa, 10–14 May 1994, Proc., Trans. Tech. Publ. Aedermannsdorf 1994.
- 12 F. W. Poulsen, G. Lauvstad and R. Tunold, *Solid State Ionics*, 72 (1994) 47.
- 13 M. Bode and K. Teske, *GIT-Fachz. Lab.*, 40 (1996) 209.